Experimenting With Polymer Blend Solar Cells and Active Layer Thickness

Senior Project by,

Ryan Blumenthal

Advisor, Dr. Robert Echols

Department of Physics

California Polytechnic State University

San Luis Obispo

May 2013

Contents

ABSTRACT

Bulk heterojunction organic photovoltaics utilize the electrical characteristics of semi-conductive polymers. These solution processable materials are beneficial because of their low material cost, light weight, and simple fabrication requirements. Our devices employ multiple photoactive polymers, P3HT and PCPDTBT, to absorb photons over a wide spectral range. We optimized various device characteristics including thickness and thermal anneal usage to reach a power conversion efficiency of 3.0% in AM1.5 sunlight. Device performance degrades over time due to atmospheric water and oxygen, prompting us to investigate device packaging to extend cell lifetime for additional testing.

INTRODUCTION

This is currently a defining time in the era of energy: the scientific community now accepts as fact that global warming is indeed occurring and that it will have long-ranging impacts on the earth's ecosystems[1]. Both the government and public are starting to question the use of oil, coal and other non-renewables as our main energy sources[2]. The United States government is providing subsidies for the use of current renewable technologies and supporting research in upcoming renewable projects that may provide a cheaper, cleaner and longer lasting solution than non-renewables[2]. According a study by the United Nations, renewable energy technology has attracted more global investment than fossil fuel for the first time ever[1]. The second most invested renewable sector is solar energy [1] and research in organic photovoltaic solar cells will likely allow solar energy to increase its economic competitiveness, power efficiency and range of applications.

Organic photovoltaic (OPV) are considered to compete with silicon based solar cells which have high fabrication demands, careful installations requirements, and a relatively expensive cost[3]. Polymer solar cells, however, are aimed to be lightweight, thin, mass producible, and cheap[4]. For example, some companies have successfully printed OPV cells on plastic to offer many applications thanks to its flexible medium[4]. A paper estimating the impact of OPV cells shows that they have the potential to reduce the cost of solar electricity by fourfold[4]. However, OPV cells must overcome efficiencies of 5% and a lifetime of 10 years if they are going to become economically competitive with non-solar energy[4].

Our research in polymer based solar cells hope to increase the efficiency in these devices to help them become more viable in the future. We experimented with the thickness of the photo-active polymers to optimize their efficiency. With these results, future OPV production could manufacture cells to this specification to reach optimum energy production. Realistically, these results help further understand the mechanics and materials inside OPV cells for further research.

EXPERIMENTAL DESIGN

The essential mechanism behind polymer based solar cells is creating current from an absorbed photon inside a polymer. A photon has a discrete energy and can excite an electron to a higher energy if absorbed. If the molecule's band gap energy is similar or less that of the photon, the photon can excite an electron from the highest occupied molecular orbital (HOMO) to the lowest unoccupied molecular orbital (LUMO)[5]. Making an effective active layer polymer requires that we find or match the electronic band gap energy to that of the spectrum of light from the sun. In this way, we maximize the devices' ability to convert solar energy to electronic current.

The active layer of OPV cells is comprised of an electron-rich photoactive polymer willing to give up electrons when it absorbs photons. However, polymers have a fixed energy band gap that will limit their absorption spectra. In this experiment our active layer was comprised of different blends of poly(3-hexylthiophene) (P3HT) and Zhengguo Zhu's PCPDTBT (ZZ50)[6] in order to maximize the absorption spectra. As seen in figure 1 below, the different band gap structure of ZZ50 and P3HT harnesses different areas of the solar spectrum. Since our polymers can only convert one photon to one electron, it is important to harness the as much of the solar spectra as possible. The photon with more energy will not yield more energetic charges since a photon can only transfer the energy difference between the polymer's HOMO and LUMO levels at best. Thus, it is important to be unselective when trying to capture a region of the solar spectra; the ideal device would be able to absorb all photons that have high enough energy to excite the electron.

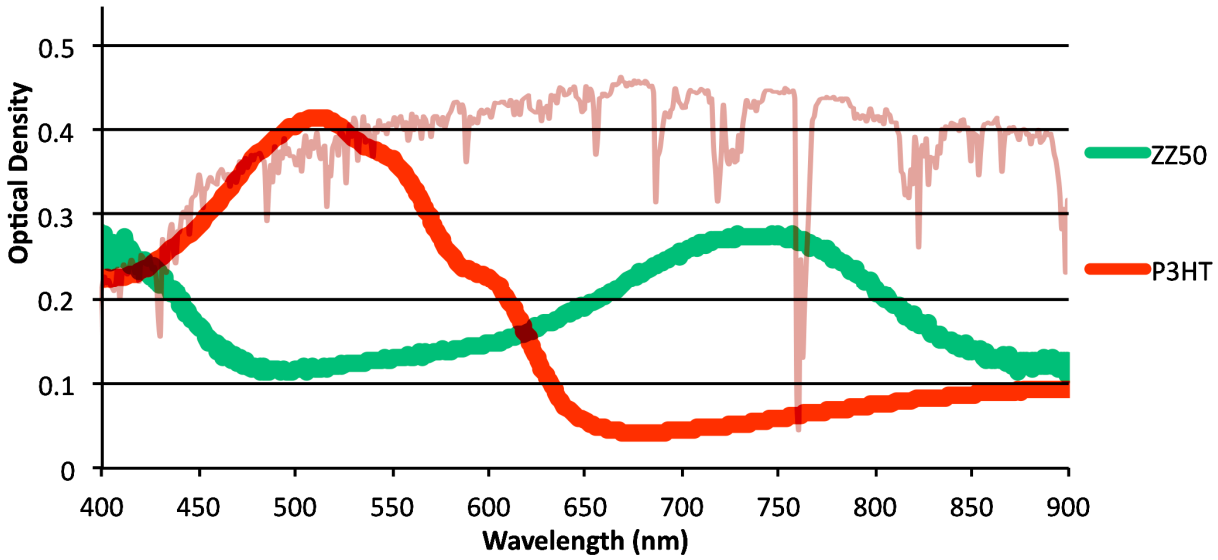

Figure 1: Different absorption spectra of P3HT and ZZ50. The background spectra is photon flux per wavelength coming from the sun[7].

After a photon enters the active layer polymer, it might be absorbed in one of the photoactive polymers: P3HT or ZZ50. This absorption event of the photon creates an exciton: a temporarily excited electron and a positively charged hole from where that electron came from. Under normal conditions the exciton would collapse in less than 1 ns[8]. However, another molecule, (6,6)-phenyl-C61 butyric acid methyl ester (PCBM), is blended with the electron rich photoactive polymer to be an electron receiver and transporter[8]. In contrast to the above timescale, the process of transferring the electron to the PCBM occurs at about 45 fs allowing for excitons to be split before they recombine[8]. As seen in figure 2, PCBM (n-type material) will remove the excited electron from the polymer and provide a pathway for the electron to the cathode. The PCBM molecules are a necessary component to the design of the bulk heterojunction active layer and must be included in our polymer blends. In our experiment, we used a blend of P3HT and ZZ50 in the following ratio: 16 P3HT : 16 PCBM : 4 ZZ50 mg/ mL solvent. P3HT and ZZ50 work together to extract the holes as our p-type layer.

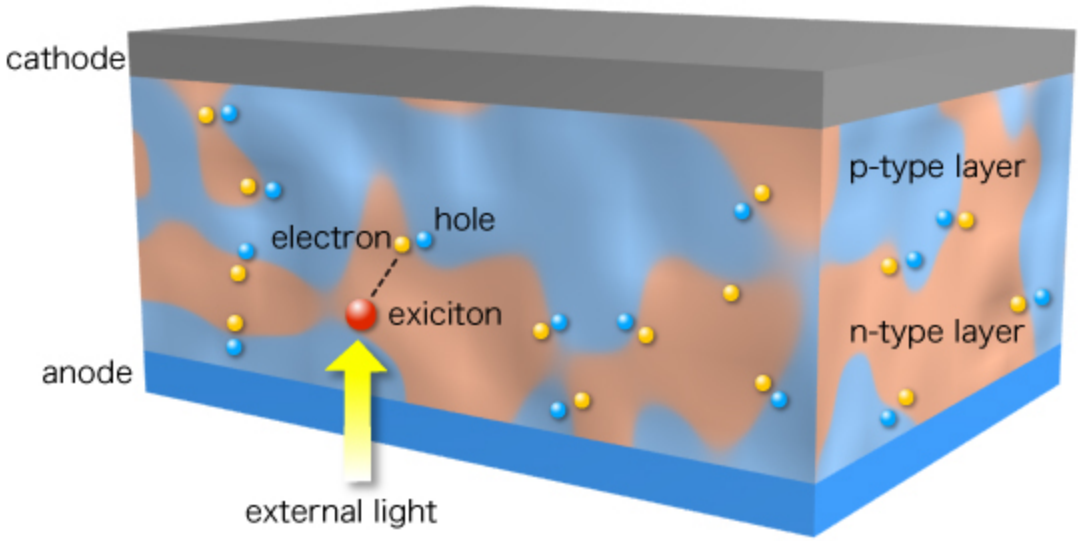

Figure 2: Bulk heterojunction containing p-type layer of active polymer and n-type layer of PCBM[9].

The active layer, as mentioned before, works by the combination of the electron donating polymer and the electron accepting PCBM. This means that the electron donating and accepting materials are highly intermingled as to allow abundant surface contacts for the exciton pair to separate. Much study has gone into the bulk heterojunction because it is critical that there is enough surface area to separate the exciton pair within 1 ns but also large enough phase regions to transport the charge to the electrodes[8]. Unfortunately, we have little control over the bulk heterojunction morphology at the time of spin coating because it is important that the polymers are properly dissolved in solvent. At this stage, the choice of solvent is the most influential factor in morphology. If the polymers and PCBM are too intermingled then charge extraction becomes

difficult; complicated conduction paths causes charges to be lost and power lost. For this experiment, we varied the thickness of the active layer to observe the effects of charge extraction and absorbance to find an optimized layer thickness based on maximizing efficiency.

To enhance the morphology of the active layer, we thermally annealed the devices. From past research, we expect the anneal to improve the crystal quality of the film and help order the bulk heterojunction[10]. Annealing the devices after the active layer has been spun on gives thermal energy to the polymer molecules and allows molecular mobility within the film. This allows the molecules to find a chemically favorable composition which is a less mixed configuration. This forms more distinct crystals and phase regions and interpenetrating networks within the active layer[11], a process named spinodal decomposition. Figure 3 demonstrates the importance of a more ordered heterojunction: the conduction pathways are easier to navigate, longer and less ending paths in a less mixed active layer. This increases the amount of separated exciton charges able to get to the electrodes, but it may also hurt our ability to separate the exciton pairs if there is significantly less surface area between our n-type and p-type materials. However, research shows that the conduction improvements in the bulk heterojunction vastly enhance the efficiency[11].

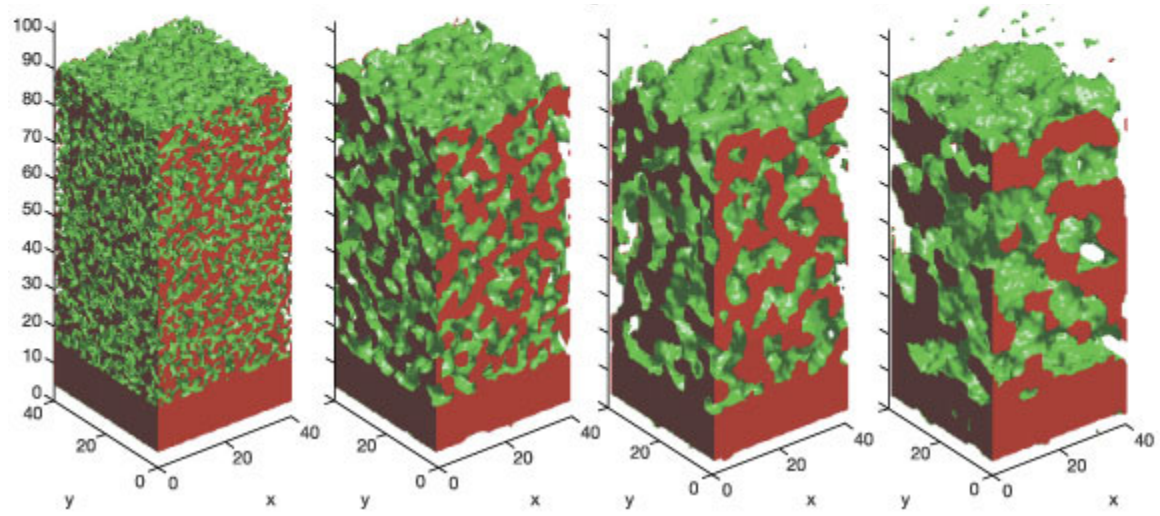

Figure 3: Changing morphology of the bulk heterojunction by annealing the devices. The left is the visualization of our solution when it is applied and the right is a visualization of a more ordered heterojunction[12].

The rest of the device architecture is designed to separate the charges to create current. A diagram of the cross section of the device is demonstrated in figure 4. We use a glass substrate with rectangular sections of transparent Indium Tin Oxide (ITO). The ITO is the anode on our device, but it is relatively fragile and susceptible to deterioration. However, it is useful for its high transparency, conductivity and relatively high work function[11]. A layer of poly(3,4-ethylenedioxythiophene):poly(styrenesulfonate) (PEDOT:PSS) is spun on top of the ITO. The PSS dopes the PEDOT making it more conductive and soluble in water. The PEDOT:PSS layer

itself improves hole extraction from the active layer[10]. On top of the active layer, a thin layer of aluminum is deposited to act as the electron transport layer. This layer acts as the cathode and is applied with a thickness of about 100nm. Also using varying areas of aluminum cathode allows us to change the area of our pixels. The electrode materials, photoactive polymers and charge carriers are all chosen due to their individual energy levels.

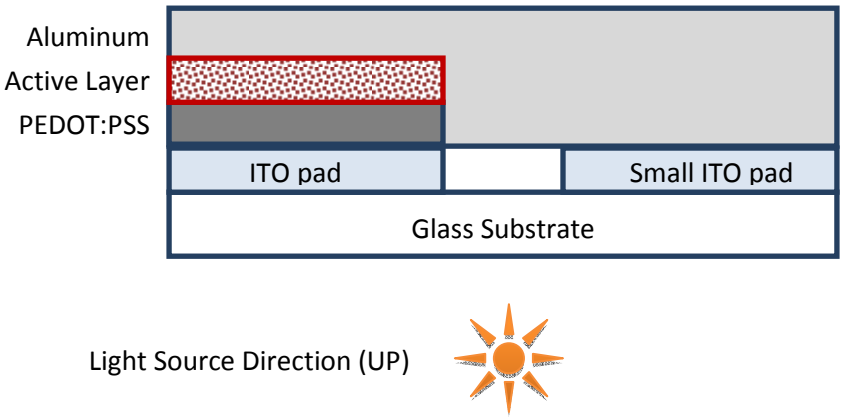

Figure 4: Device architecture

To extract current, the hole and electron, arising from an exciton split at a polymer/PCBM boundary, must travel to the electrodes. This is only possible if there is a built in electrical bias which comes from the energy level separations between P3HT or ZZ50 and PCBM. The energy diagram is illustrated below in Figure 5. An excited electron shown starting from the P3HT LUMO level will jump to the PCBM LUMO level due to the energy level favored difference between them. From the PCBM, the electron will jump to the aluminum cathode once it has travelled to the junction between the materials. The hole travels to the ITO electrode by first jumping from P3HT, to PEDOT, then to the ITO. The overall internal bias primarily set from a difference in electrode work functions allows for power to be extracted. The energy level difference between the LUMO level of the PCBM and the HOMO level of the photoactive polymer is the maximum possible open circuit voltage (V_{oc}). This voltage partially defines the highest achievable power conversion possible. The polymers are carefully chosen to define the device's V_{oc} while also preserving the electron and hole extraction bias.

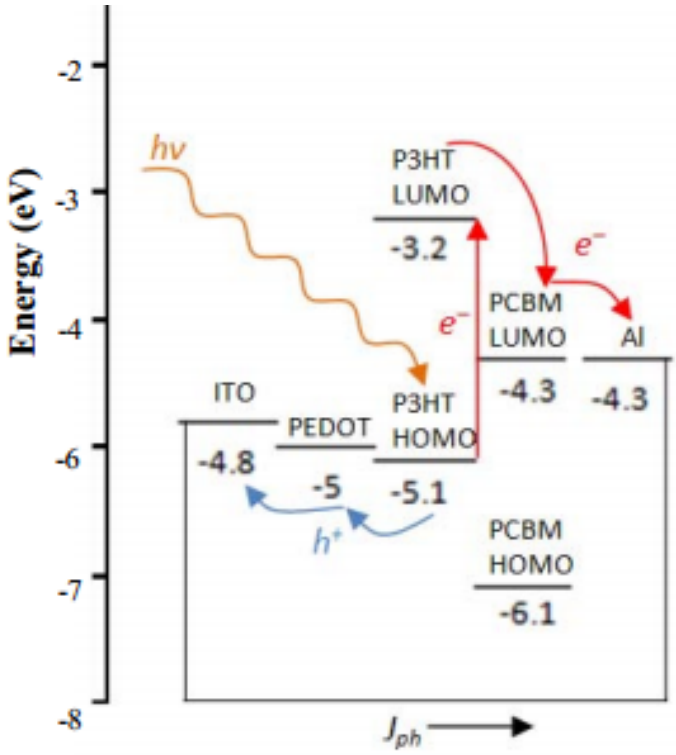

Figure 5: The energy level diagram of P3HT and PCBM in contact that illustrates the built in bias used to extract charge[13].

DETAILED PROCEDURE

To create the architecture seen in Figure 4, we will start with the glass/ITO substrate and work our way up. It is important to clean the substrates to eliminate particles, contaminates, and imperfections that could hinder device performance. In the fume hood, we put 12 substrates into a substrate holder and to prepare them for solvent baths. The first bath is an acetone bath because acetone's a powerful solvent for removing organic particles. The substrate holder is placed into an acetone filled beaker, put into an ultrasound bath and then run for 3 minutes. The ultrasound bath gives more energy to the solvent molecules to aid removing impurities from the surface. After the acetone bath, the substrates are removed and dried with a nitrogen air gun. The substrates then undergo another round of cleaning using isopropyl alcohol and another 3 minutes in the ultrasound bath. Isopropyl alcohol is good at removing polar particles from surfaces and rinsing off acetone residue. After they are dried with nitrogen gas again, we have hopefully cleaned off any microscopic particles. We transfer the substrates in the substrate holder to the dust free area while applying a steady stream of nitrogen gas. This helps keep dust off or prevent dust from settling on the surface of the substrates while transferring to the dust free zone. The substrates are stored in the UV ozone machine to further dry with the ITO surface facing up (UP direction).

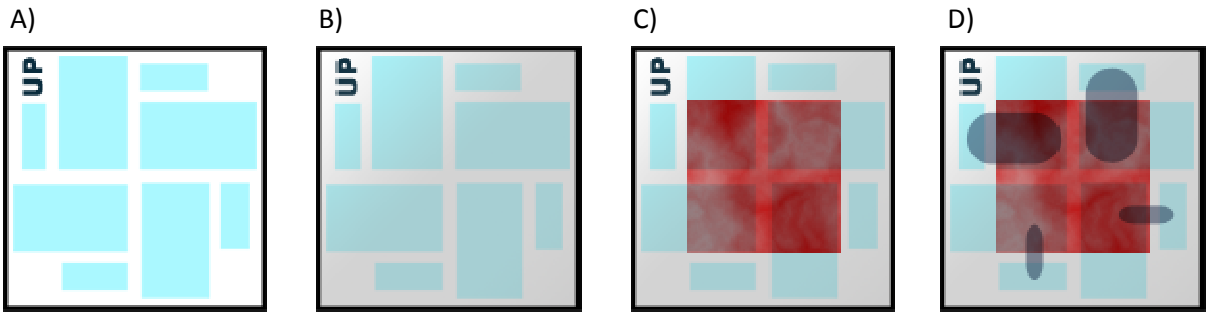

Figure 6: Demonstrating the step by step procedure to create a device. A) The cleaned substrate with patterned ITO, B) The PEDOT applied everywhere, C) The active layer applied and swabbed, D) The aluminum cathode applied to each pixel to complete the device.

When the substrates have dried and the lab is prepared for the next step, we turn on the UV ozone machine to prepare the anode of the device. The UV ozone helps remove microscopic organic particles, but it also increases the performance of the ITO. The UV ozone machine increases the surface concentration of oxygen on the substrate and also raises the work function of the ITO[11]. Immediately after the UV ozone completes, we work individually with the substrates and put them on the spin coater with the ITO facing up. We start the procedure to apply the next layer immediately after the UV ozone machine completes because we want to trap the surface oxygen and surface wetting is improved. We apply PEDOT:PSS (usually abbreviated as PEDOT) dissolved in water with a filtered pipette to stop any solid PEDOT from getting onto the substrate. Solid PEDOT is not useful for the thin layer and is likely to leave undesirable streaks from the spin coating. The substrates are spun with PEDOT:PSS at 5,000 RPM for 1 minute and then removed. Then with a wet cotton swab, we swab away the outer PEDOT that connects the small and large ITO pads. This prevents electrical shorting and leakage in the device. Water is the solvent for the PEDOT and now must be removed because it would interact with the active layer and contaminate the glove box. The substrates are immediately annealed for 15 minutes at 125^{o}C to remove the water. After the anneal, the substrates are transferred into the glove box. The anode layer is now complete and ready for the active layer. In summary, the PEDOT layer acts as a diffusion barrier to trap the oxygen with the ITO for improved performance, improves wettability for the active layer, and improves hole extraction from the active layer from its high work function.

Inside the glove box, a solution of photo-active polymers and PCBM is prepared. The blend ratio of 16 mg P3HT : 16 mg PCBM : 4 mg ZZ50 / mL solvent is combined with 2 mL of chlorobenzene in a bottle to dissolve them. The beaker is placed on a hot plate at 50^{o}C and with a spinning magnetic stirrer to help break down the solid polymer. The substrates are placed on a spin coater with the UP direction facing up. The polymer is applied to the substrate with a pipette

carefully as not to scratch the PEDOT layer. Each substrate is spun at various spin speeds for 40 seconds and then taken out of the spin coater. The spin speeds RPM range for these experiments are 650, 1000, 1500, 2000, and 4000. Carefully holding the substrates at a downward angle, we swab away the outer region of the active layer that overlaps the ITO pad with tetrahydrofuran (THF). This is done to connect the following aluminum layer to the small ITO pads. For testing, we simply need to connect contacts to each ITO pad to complete the circuit and provide good electrical contact (see Figure 6C and 6D). Yet even with the active layer applied, the final electrode must be added before the device is complete.

The substrates are transferred over to the "evaporation" glove box where the aluminum electrode is applied. The substrates are laid on top of a masking stencil that creates the preferred shape of the cathode for each pixel. This allows us to create pixels of two different sizes: two small pixels of 3.75mm^2 and two large pixels of 42mm^2. Figure 6D shows the relative sizes and shape of the 4 pixels located on each substrate. A bell jar lowers over the chimney where the substrates are housed. A roughing pump lowers the pressure in the jar and then we used a diffusion pump to reach very low pressure of $1x10^{-6}$ Torr. The aluminum in the boat is evaporated by running large currents through it. The evaporated aluminum will deposit a thin layer of about 100 μm thickness. This process occurs under extremely low pressure to ensure line of sight deposition through the mask and that the aluminum particles will not interact with any gas molecules.

Next the substrates are tested in the testing station. The devices are loaded into a testing jig where the light's input power is calibrated. A Keithley applies a voltage at .05 V intervals and measures the current outputted by the device. Each pixel was measured in this process in both light and dark conditions. We test the devices immediately after the aluminum treatment. Later, the cells receive a thermal anneal of 105^{o}C for 30 minutes. The tests are repeated to observe the effects of the anneal. Testing includes JV analysis of the current and an optical density (OD also called UV-Vis) to measure absorption characteristics. Devices are then packaged using aluminum tape and are sealed with epoxy around the edges. Although this is not industry standard packaging methods, it allows us to further test the cells out of the controlled conditions of the inert nitrogen atmosphere glove box. Once the devices are pulled out of the glove box, they are tested in AM 1.5 sunlight conditions of 1000 W/m^2 and tested for external quantum efficiencies (EQE).

ANALYSIS:

The data from the Keithley is saved and analyzed for all solar cells. Using matlab, I can plot the data and use scripts to automatically find important data. A good solar cell should behave like a diode and it is easy to qualitatively determine the effectiveness of a solar cell by looking at a plot of the data. This idea is demonstrated in figure 7. The efficiency is really determined by its max power point: the point where (current)x(voltage) is maximized. This point can be found easily using a script and is highlighted in figure 7 by a red dot on the curve.

Estimating the positions of these two stars on the graph should give an idea for how efficiency increases for a cell performing like a diode. Efficiency is formally calculated by taking the max power point, normalizing by area and then dividing by input power.

$$Power\ conversion\ efficiency\ (PCE) = \frac{Power\ out}{Power\ in} = \frac{P_{max}}{Area * Intensity\ \frac{W}{m^2}}$$

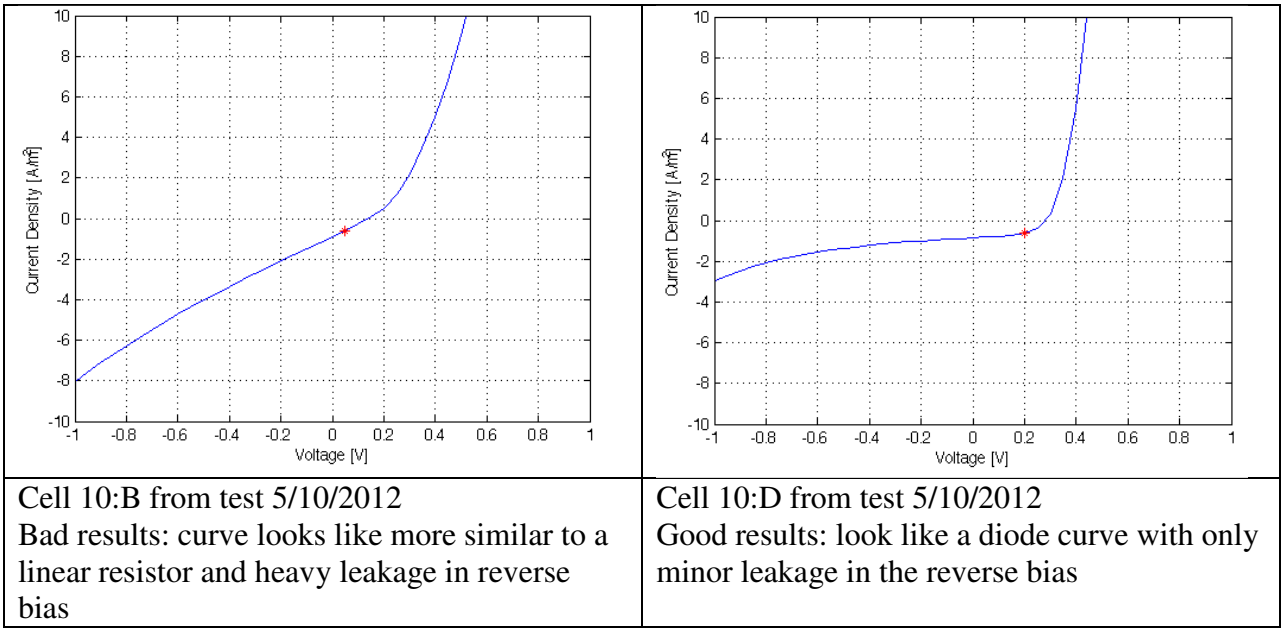

Cell 10:B from test 5/10/2012 Bad results: curve looks like more similar to a linear resistor and heavy leakage in reverse bias	Cell 10:D from test 5/10/2012 Good results: look like a diode curve with only minor leakage in the reverse bias

Figure 7: Qualitative pixel comparison to determine solar cell effectiveness

Another important metric to calculate is fill factor (FF). Fill factor is a measurement of charge extraction efficiency based on the comparison between the max power point and the potential maximum power. The equation for fill factor is given below:

$$FF = \frac{JV_{max}}{J_{sc}\ V_{oc}}$$

where J_{sc} is the short circuit current density with no voltage bias and V_{oc} is the voltage bias required to make the current 0. Fill factor ranges between 0 and 1. It is a useful metric to quantitatively measure charge extraction properties and can be thought of as charge extraction efficiency. We can use these properties of fill factor, conversion efficiency and absorption to study the effects of annealing.

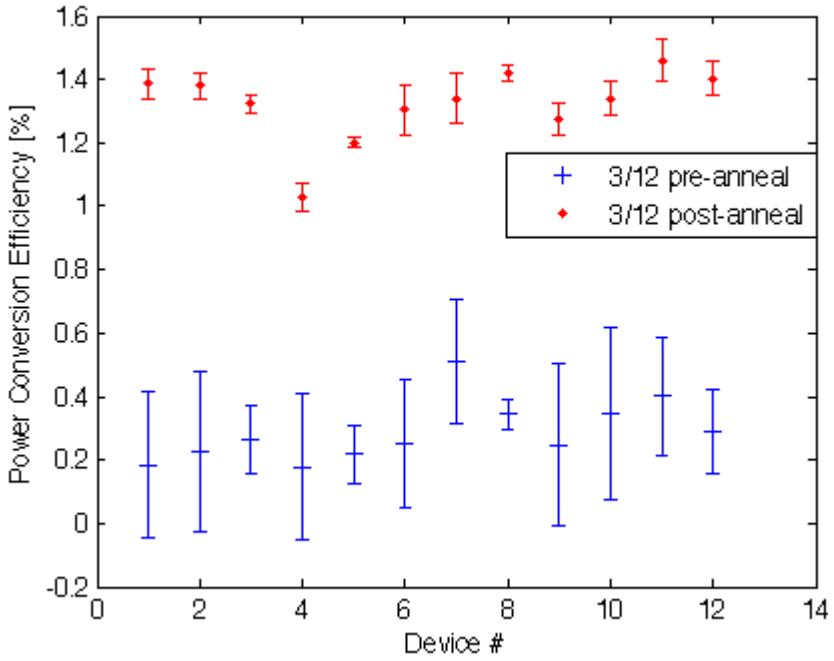

Figure 8: Efficiency change from thermal anneal in low light conditions (approximately 18 W/m^2). Each devices' 4 pixels were averaged together and the standard deviation was used for the uncertainty

A thermal anneal, as explained in the experimental design, alters the morphology of the active layer. We can measure and observe the effects of this in several ways. Perhaps the most important quality to investigate first is the PCE. In figure 8 above, we can see that the anneal uniformly improves all devices. The 12 devices in figure 8 have a variety of thicknesses, yet all improve by a comparable amount. All devices benefit from an efficiency improvement by roughly a factor of 4. Efficiency is our main goal of improvement and optimization, and a thermal anneal clearly benefits the device performance. We'll also investigate the mechanics behind the cause of this improvement within the device.

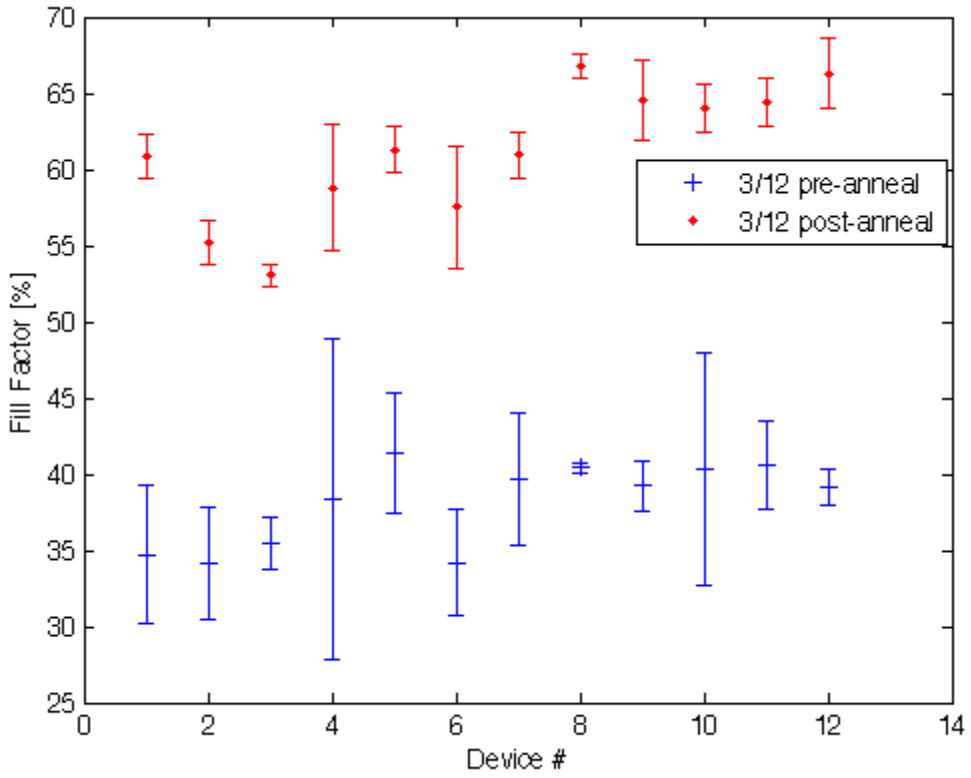

Figure 9: The effects of a thermal anneal on charge extraction

As discussed in the experimental design, we expect the thermal anneal to increase charge extraction characteristics through spinodal decomposition. As the polymers and PCBM separate and form more distinct regions, the conduction paths become larger and easier to navigate. Figure 9 demonstrates these changes in charge extraction. We can see an average improvement of 50%. However, why the charge extraction improves is actually a bit more difficult to explain when considering OD tests.

One of the main benefits of annealing is the improvements on the optical properties. The OD testing shown in figure 10 illustrates the optical changes in the device. Without changing the device's thickness or its architecture, thermal annealing allows the device to absorb more photons! This is caused by the P3HT crystalizing and ordering itself when given thermal energy[11]. The creation of the shoulder at roughly 600nm in the P3HT peak supports the case that the P3HT is crystalizing[11]. Crystalized P3HT also greatly improves charge mobility and the exciton diffusion distance which is the distance an exciton can travel before it recombines[11]. Therefore, the crystalized P3HT benefits from more absorption events, more excitons being separated, and more conductive charge pathways all due to the thermal anneal. The ZZ50 does not see these benefits as it remain amorphous and does not crystalize. However, the spinodal decomposition of the bulk heterojunction benefits both polymers by creating a better charge carrier network. Unfortunately, the ZZ50 has a slight decrease in absorption from the thermal

anneal as well. Although, the amount absorbed is still greatly increased overall when comparing both peaks. Lastly, both peaks are slightly red shifted. Notably, the P3HT peak is shifted by almost 30 nm. This does not hamper the device performance but it can be viewed as a characteristic feature of annealed devices.

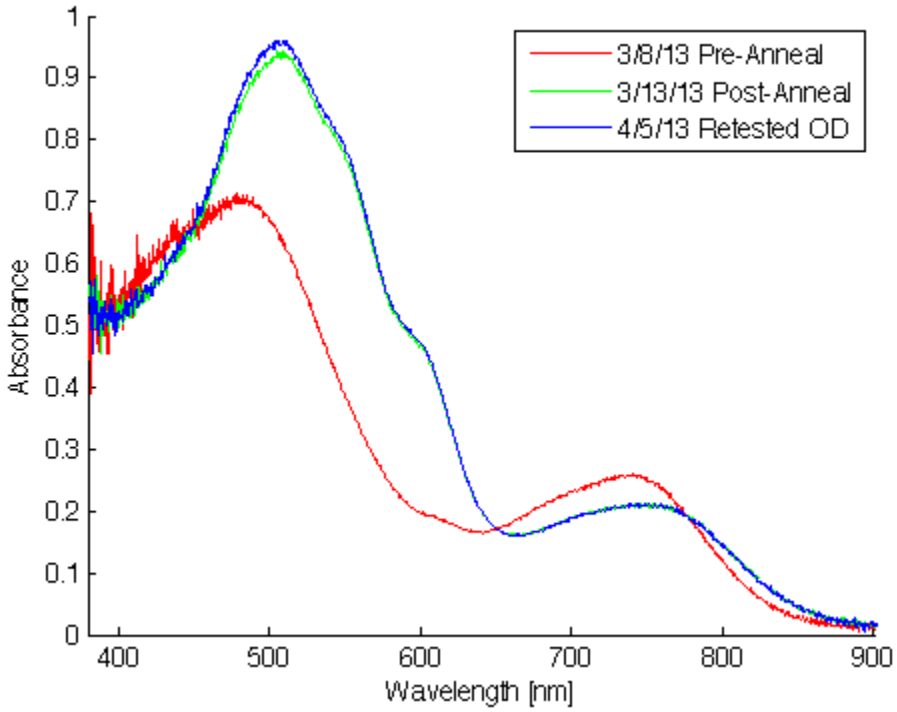

Figure 10: The optical effects of annealing on a 650 RPM polymer spun device.

Next, we setup an experiment to investigate the optimized active layer thickness of these devices. Active layer thickness is one of the key optimization techniques used to create more efficient devices because it finds the best combination between charge extraction and absorption. Thicker devices have more material the photon travels through providing more absorption events. Thinner devices, however, have stronger charge extraction capabilities due to the complexity of the bulk heterojunction and a larger internal electric field. A thicker active layer means that the complicated charge extraction network must be longer and therefore more difficult to transport charges without loss. Using the exact same fabrication methods for all devices, we did a preliminary run using different polymer spin speeds of 1, 2, and 4 kRPM. Each spin speed group had 2 devices with 4 pixels per device to test. We tested these devices for absorption, charge extraction and efficiency.

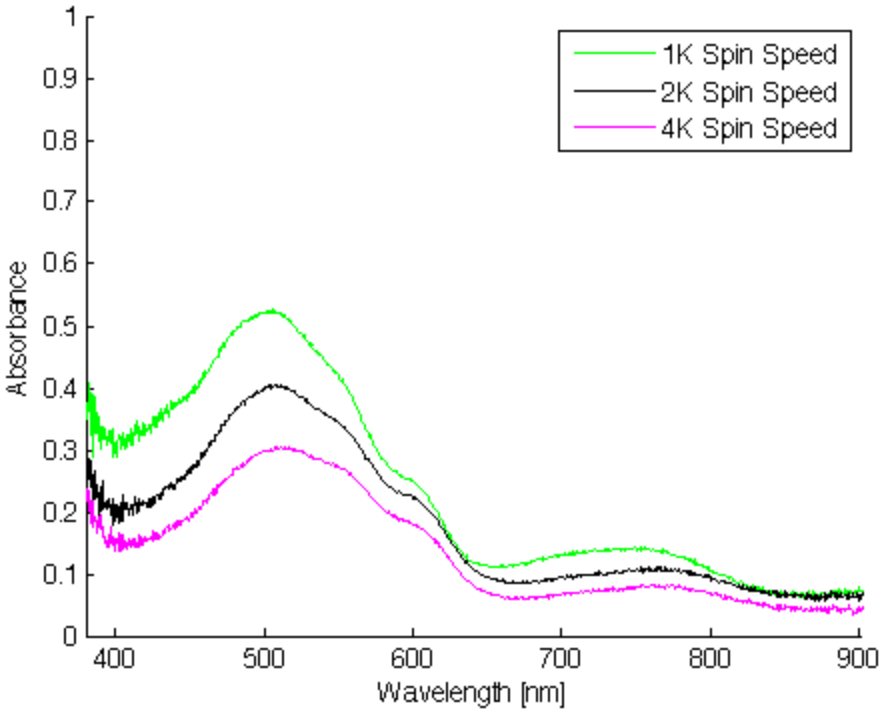

Figure 11: Absorbance analysis illustrating the effects of active layer thickness. These are post-annealed devices.

Absorbance is equal to absorptivity multiplied by distance (thickness), thereby thicker devices have linearly larger absorbance. Figure 11 shows that the thicker devices do absorb more light across the spectrum. We can also see that our 1K device has nearly twice the absorbance than the 4K device. More absorbance means more captured photons and therefore more excitons generated. This graph is a great example of the increased absorption benefits with a thick active layer. These devices are post-anneal treatment as seen by the characteristic P3HT crystallization bump. Furthermore, we examined charge carrying capabilities of these cells to see how they compare.

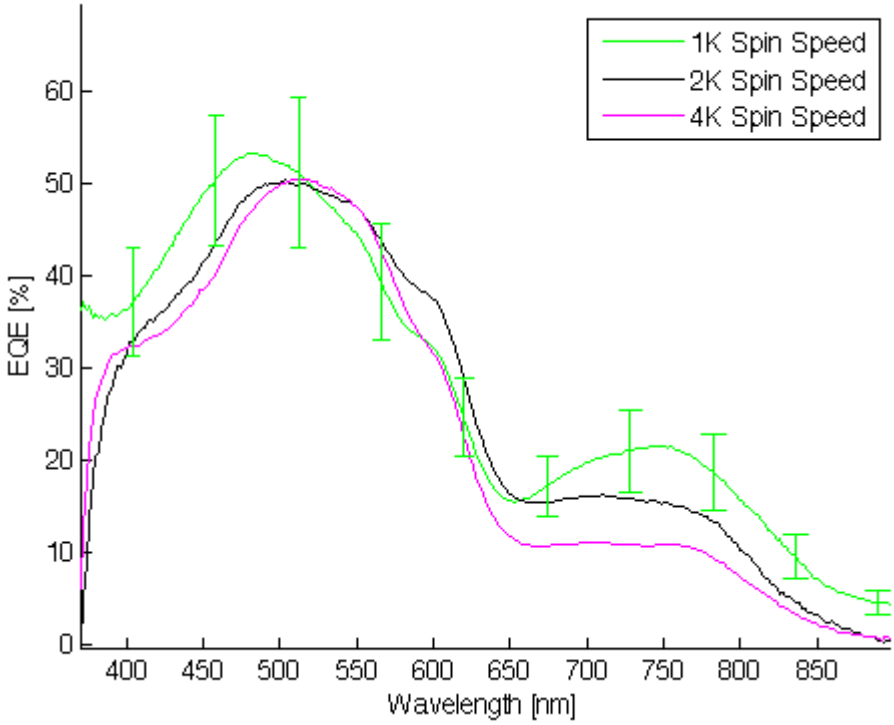

Figure 12: External quantum efficiency as a function of wavelength at three spin speeds. The uncertainties are the standard deviations of all the pixels in a device group

Another test we conducted to characterize these devices is external quantum efficiency (EQE). EQE is another efficiency ratio ranging from 0 to 1 of incident photons to converted electrons. This ratio is calculated by measuring the J_{sc} and dividing by the intensity of light times electron charge at a fixed wavelength interval. The light reading is taken from a calibrated photodiode. A monochrometer controls the wavelength of light allowing us to determine the devices' electrical performance as a function of wavelength. The equation to calculate EQE is given below:

$$EQE = \frac{J_{device}}{J_{diode}} * EQE_{diode}$$

The results of this measurement are plotted in figure 12. The lines are the average EQE for each of the 4 pixels for one device. I've also added the uncertainty in the measurement to the 1K device which was measured by calculating the standard deviation between the 4 pixels. The point of the uncertainty is to show that the 1K devices have slightly higher EQE measurements than the 2K devices on average, but statistically agree due to uncertainty. However, the 1K devices register higher than the 4K devices in the ZZ50 spectral region. This is curious considering the P3HT region of the EQE seems to be independent of thickness while the ZZ50 region is more dependent on thickness. Overall, ZZ50 seems to perform better in relatively thicker devices.

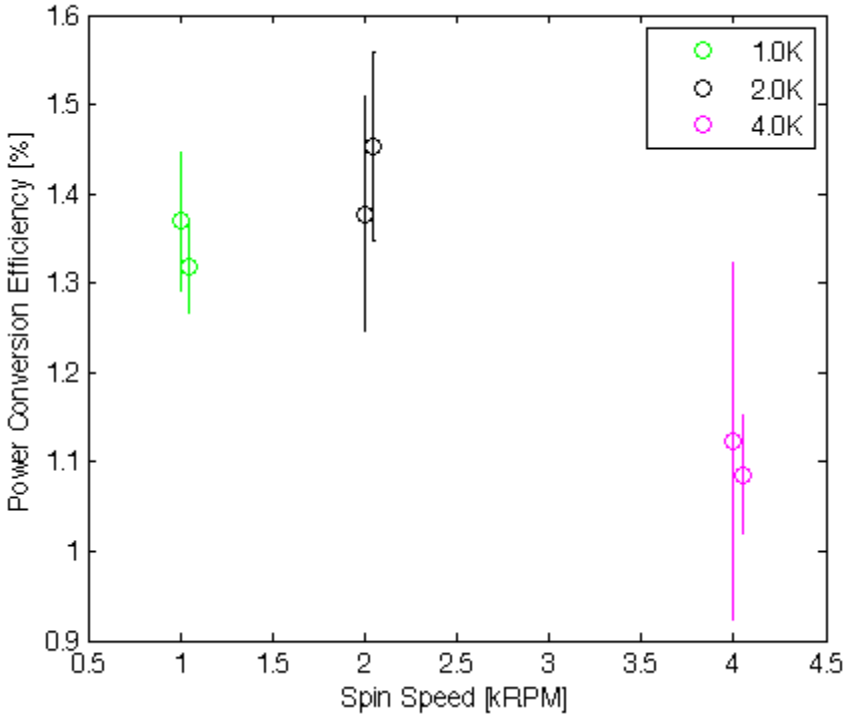

Figure 13: Power conversion efficiencies of several devices under low intensity, 18 W/m^2 illumination

Device performance can be primarily measured in power conversion efficiency, which is the goal of our optimization. In figure 13, we can see the preliminary optimization results. Although there aren't enough devices in each group or enough spin speed groups to notice a large optimization point, we can see a region of interest in the lower spin speeds (thicker devices). The 1K devices are more tightly grouped, yielding better uncertainties. The 2K devices have slightly higher efficiencies on average than the 1K devices but wider uncertainties. Lastly, the 4K devices show lower performance on average and wide uncertainties. However, these results hinted that there may be an optimization region within the 1K-2K area of spin speeds. To further investigate this idea, we setup another experiment similar to the last. We changed the spin speed groups and the number of devices to target for more significant results. For the second experiment, we used spin speeds of 0.65K, 1K, 1.5K, and 2K with three devices per group. We used the 1K and 2K groups as a double control to verify the comparison drawn in figure 13. We also decided to use .65K instead of 2.5K because thicker devices have potential for greater efficiency. We were hoping to find a thick optimization peak and wanted to include a wider search parameter just in case. Working with 12 devices total, we should be able to make statistically significant conclusions with an added device per group.

After these devices were fabricated, we again performed optical, charge-extraction and JV testing on them. Looking at the optical data plotted in figure 14, the data again has the

absorbance ordered by relative device thickness. The 0.65K devices have an absorbance of roughly 1, which corresponds to 90% of the incident light to the active layer absorbed. This type of optical absorbance is quite desirable in a fully working device. By comparison, the 1.5K device has an absorbance of about 0.5 which corresponds to 68% of light absorbed. Thick devices seemingly have a large advantage over thin devices because of the significant amount of additional light absorbed and excitons produced in the active layer. However, investigating these slow spin speeds also allowed us to see the thickness correlation to charge extraction.

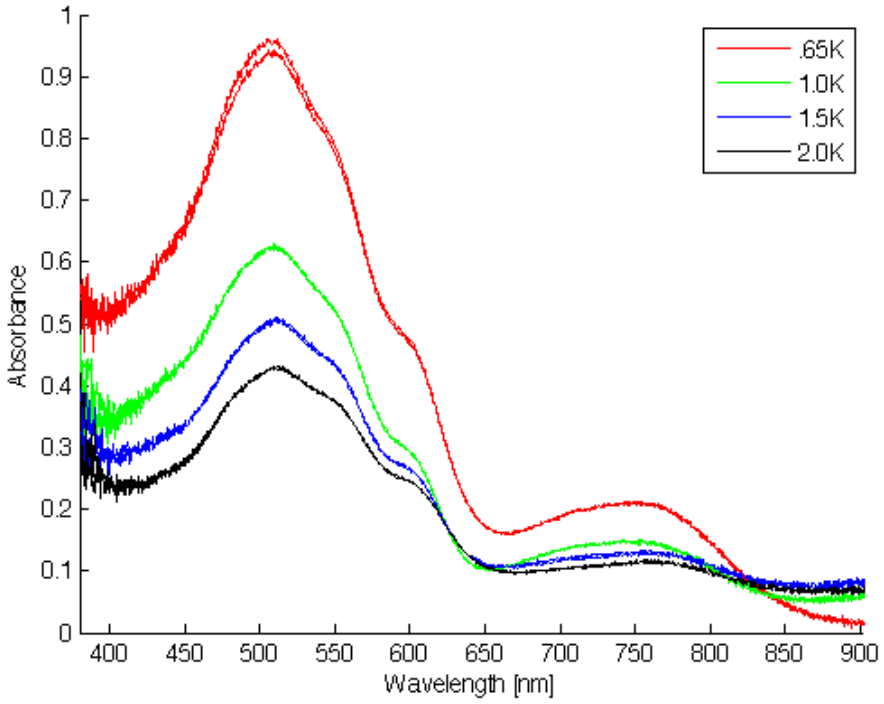

Figure 14: Absorbance of several different thicknesses tested after annealing. Each color has two pixels from a device to show relative uniformity

To examine the devices electrical properties, we again turn to fill factor as an estimate of charge extraction and resistive losses. Figure 15 shows the fill factors of each device group corresponding to their thickness. We can see a correlation between spin speed and fill factor. The results of this tell us that thinner devices are extracting charge better. Increasing the active layer thickness and consequently the charge travel distance in this network seems to hurt the devices ability to extract charge. Also, thicker devices have the same internal voltage due to the same material work functions as thin devices, but electrons feel less of an electric field due to the increased distance between electrodes. It appears the thin devices have greater fill factors, which would directly correlate to better efficiency if thinner devices absorbed the same amount of light as thick ones. However, there is a compromise between thickness and charge extraction that we can directly see in comparing the results in figure 14 and figure 15. Thinner devices absorb significantly less light but extract the charges that are created much more efficiently.

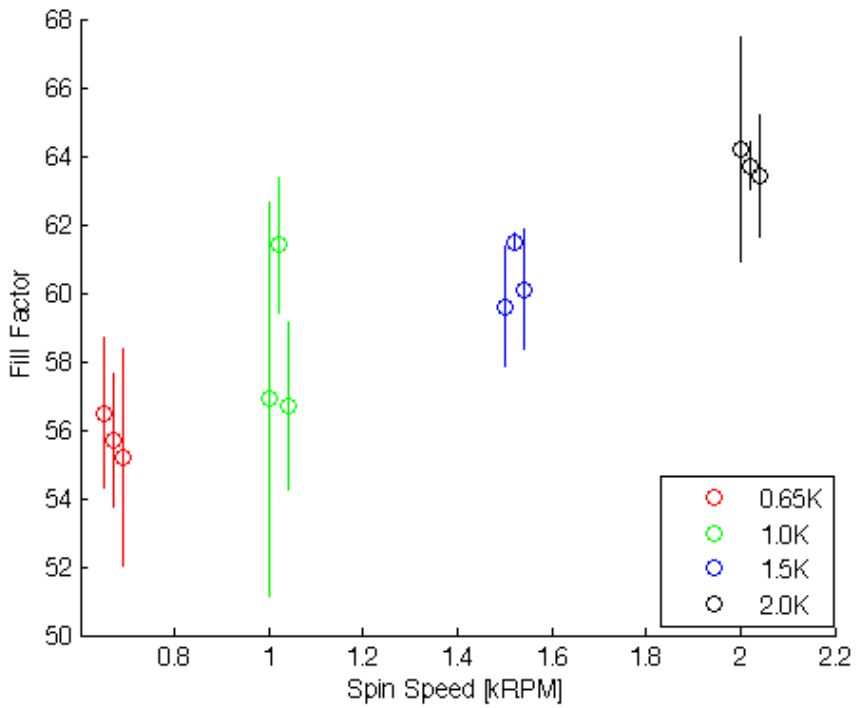

Figure 15: Fill factor dependency on thickness. These measurements were taken for packaged devices illuminated in AM1.5 sunlight to consider realistic deployment conditions. Uncertainties are the standard deviations between all pixels on a device

Now to consider the combination of charge extraction and absorption: power conversion efficiency. The results of our sunlight testing are plotted below in figure 16. The single packaged device from the last experiment was also added to the plot to give a comparison to very thin devices. We can see an interesting trend where the 4K device and the 0.65K devices have comparable efficiencies. However, the devices in between these groups follow a peak curve due to the optimization of charge extraction and absorption. In this test, the 2K devices have the highest power conversion efficiencies on average. The best pixel on the best substrate recorded a PCE measurement of 3%, which is quite high considering the average of all the pixels from all devices was 2.1%. From these results, we can conclude that a spin speed of 2,000 RPM was the best out of the tested spin speeds. More testing may need to be done to statistically prove that the 2K devices are always better than the 1.5K devices. This hesitation comes from the overlapping measurements within these two groups and most of the data being in agreement within the uncertainty.

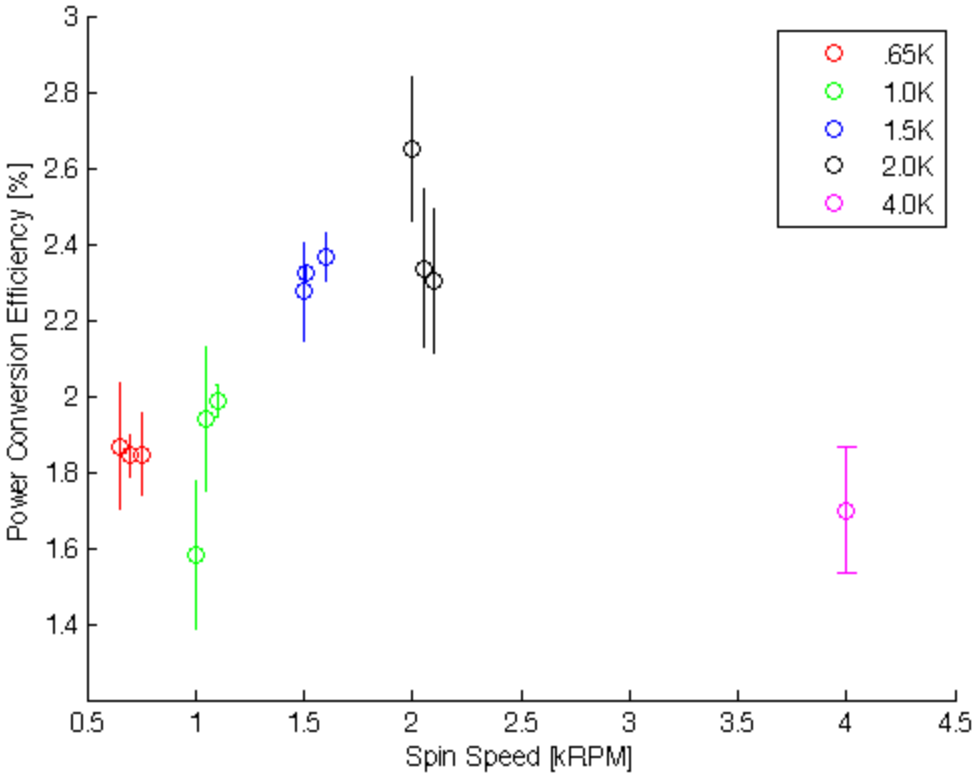

Figure 16: Power conversion efficiency dependency on spin speed. These measurements were taken for packaged devices illuminated in AM1.5 sunlight to consider realistic deployment conditions.

The last thing to consider is our device performance over time. This testing is usually referred to as lifetime testing because we test their electrical characteristics until the cells are essentially non-functioning. We designed an experiment to compare our packaged devices with aluminum tape and epoxy sealant against unpackaged cells. We tested device PCE, fit the data to an exponential decay and then plotted the results are shown in figure 17. We can see that packaged cells have a significantly longer mean lifetime. The active layer is vulnerable to degradation effects in the presence of oxygen and water. Specifically, P3HT will undergo irreversible photo-oxidation of the polymer in the presence of oxygen and light[14]. Although our method is not research standard or industrial grade technique, our technique does extend lifetime to the order of a few days. This allows one to conduct several tests without the harsh time restrictions that unpackaged cells require.

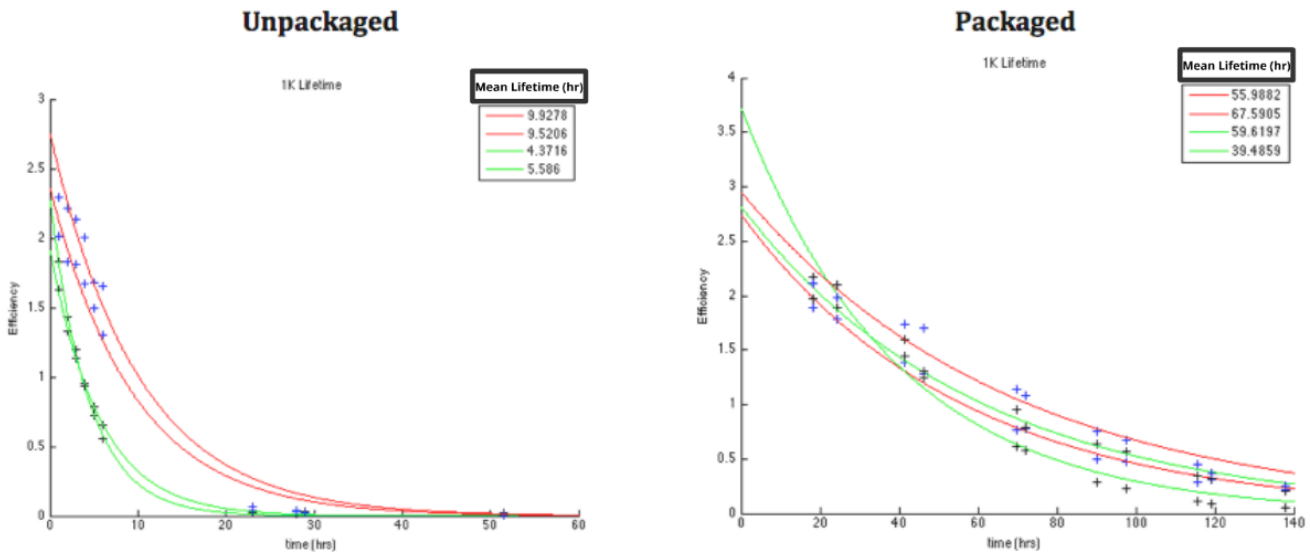

Figure 17: Importance of packaging and device sensitivity to atmospheric effects[15]

CONCLUSIONS

Several conclusions can be drawn from these experiments which provide insight into fabricating organic solar cells. First, in agreement with previous research, a thermal anneal enhances the performance of cells containing P3HT[11]. The charge extraction, absorption and power conversion efficiencies are all improved. In all cases and spin speeds, the anneal red shifts the absorption peaks in the P3HT and ZZ50. The anneal greatly improves the absorption of the P3HT through crystallization of the polymer but has adverse effects to the ZZ50 absorption peak. In short, the 105^{o}C thermal anneal for 30 minutes applied to all devices improved all these characteristics regardless of thickness. Therefore, the evidence supports the use of anneal treatment on bulk heterojunction cells containing P3HT.

The experiments on active layer thickness for a polymer blend of 16 mg P3HT : 16 mg PCBM : 4 mg ZZ50 / mL solvent revealed interesting results. The devices with a 2,000 RPM spin speed were the highest performing devices on average. The characterization testing on these varied spin speeds showed that thin devices benefit from good charge extraction capabilities due to less travel distance to the electrodes in the bulk heterojunction and larger internal electric fields. Thicker devices benefit from higher absorption which means that they generate more excitons. Measuring the power conversion efficiency of these devices allowed us to find a middle ground between charge extraction and absorption. Doing further measurements to improve the statistical confidence of our results and investigating the unexplored spin speeds between 2kRPM and 4kRPM may be an area of future research.

It is also important to discuss the application of these cells outside of the solar cell friendly conditions of the nitrogen filled glove box. Our packaging method did extend lifetime by about a factor of 5, which is convenient for extended testing. However, this is mostly for budget limited research to help improve results and testing time outside of the glove box. High grade packaging methods have lifetimes on the order of years. We concluded that it is important not to pull devices outside of the glove box without some protective sealant as the materials are sensitive to oxygen and water.

REFERENCES:

[1] Tasneem Abbasi, M. Premalatha, S.A. Abbasi. The return to renewables: Will it help in global warming control? Renewable and Sustainable Energy Reviews, Volume 15, Issue 1, January 2011.

[2] Michael Bastasch. "CBO: Most energy tax subsidies go toward green energy, energy efficiency". March 2013. < http://dailycaller.com>

[3] Sergio Pizzini, Towards solar grade silicon: Challenges and benefits for low cost photovoltaics, Solar Energy Materials and Solar Cells, Volume 94, Issue 9, September 2010. <http://www.sciencedirect.com>

[4] Erin Baker. Estimating the manufacturing cost of purely organic solar cells. University of Massachusetts, February 2009. < http://dx.doi.org>

[5] Haney, Paul. Organic photovoltaic bulk heterojunctions with spatially varying composition. Center for Nanoscale Science and Technology, National Institute of Standards and Technology, Gaithersburg, Maryland, 21 Apr 2011.

[6] Patrick Boland, Keejoo Lee, Gon Namkoong. Device optimization in PCPDTBT: PCBM plastic solar cells. Solar Energy Materials and Solar Cells, May 2010.

[7] Olson, Grant. "Multipolymer Interactions in Bulk Heterojunction Photovoltaic Devices". Cal Poly San Luis Obispo, June 2012.

[8] Scully, Shawn. Physics and Materials Issues of Organic Photovoltaics. Springer US, Flexible Electronics, 2009.

[9] Organic Solar Cell (OSC). Kyushu University, June 2008 <http://www.cstf.kyushu-u.ac.jp/~adachilab/research_d_e.html>

[10] Seong Kyu Jang. Effects of various solvent addition on crystal and electrical properties of organic solar cells with P3HT:PCBM active layer. Department of Materials Science and Engineering, Yonsei University, Seoul 120-749, South Korea. 14 February 2012

[11] Tao Hua, Fujun Zhang. Effect of UV–ozone treatment on ITO and post-annealing on the performance of organic solar cells. Beijing Jiaotong University, Ministry of Education. 9 January 2009.

[12] Peter Peumans. Efficient bulk heterojunction photovoltaic cells using small-molecular-weight organic thin films. Nature 425, 158-162, 11 September 2003.

[13] Steven Hawks, Emily Robertson. Fabrication and Characterization of P3HT:PCBM Bulk-Heterojunction “Plastic” Solar Cells. June, 2010

[14] Sperlich, Andreas, Hannes Kraus, Carsten Deibel, Hubert Blok, Jan Schmidt, and Vladimir Dyakonov. Reversible and Irreversible Interactions of Poly(3-hexylthiophene) with Oxygen Studied by Spin-Sensitive Methods. n.p.: 2011.

[15] Spencer Herrick. “Organic Polymer Solar Cells: The Effects of Packaging on Device Lifetime”. Cal Poly San Luis Obispo, June 2013.